Contribution No. 5983 from the Division of Chemistry and Chemical Engineering, California Institute of Technology, Pasadena, California 91125

Unusual Structural and Reactivity Types for Copper(I). Equilibrium Constants for the Binding of Monodentate Ligands to Several Four-Coordinate Copper(I) Complexes

ROBERT R. GAGNÉ,* JUDITH L. ALLISON, and D. MICHAEL INGLE

Received March 9, 1979

Equilibrium binding constants K^I were measured for the reaction $Cu^I(mac)^{n+} + L \rightleftharpoons Cu^I(mac)(L)^{n+}$, in which $Cu^I(mac)^{n+}$ is a four-coordinate Cu(I) complex of a polydentate ligand, L is a monodentate ligand, and $Cu^I(mac)(L)^{n+}$ is a five-coordinate Cu(I) complex. Equilibrium constants have been obtained for reactions between isocyanides, phosphites, CO, phosphines, and amines with a single, four-coordinate, copper(I) macrocyclic ligand complex. Reactions between CO and 12 different four-coordinate copper(I) complexes were also studied. In all cases equilibrium constants were obtained by using a simple electrochemical technique. Sampled dc polarography was used to obtain $E_{1/2}$ for the $Cu^{II/I}(mac)^{n+}$ redox couple in the absence and in the presence of a monodentate ligand L. The observed shift in $E_{1/2}$ was then used to calculate equilibrium constants. In general, five-coordination for Cu(I) was found to be favored for π-acid ligands, such as isocyanides, phosphites, CO, and phosphines. Five-coordinate adducts are apparently accessible from a variety of four-coordinate Cu(I) complexes. Tetradentate ligands which enforce a near-square-planar, yet flexible, ligand geometry for Cu(I) seem to promote five-coordination.

Introduction

The four-coordinate copper(I)–macrocyclic ligand complex **1** has been shown to have tetrahedrally distorted, square-planar

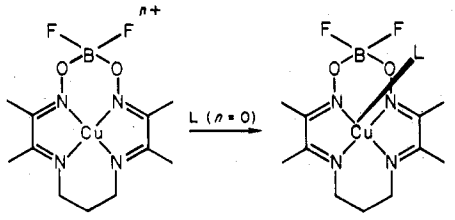

(1)

1, Cu(I), $n = 0$
4, Cu(II), $n = 1$

2

coordination.[1] Besides an uncommon copper(I) geometry, the complex also exhibits unusual reactivity, binding monodentate ligands to give five-coordinate adducts, **2** (eq 1).[2-4] The first fully characterized five-coordinate copper(I) complex, a carbonyl adduct, **3** (**2** with L = CO), was shown by X-ray structural analysis to exist in a distorted square-pyramidal configuration.[3] The carbonyl complex **3** has a copper–carbon bond length of 1.78 Å but long copper–nitrogen bonds (2.14–2.16 Å) accompanied by an extraordinary 0.96-Å displacement of copper(I) from the mean plane of the four coordinated nitrogen atoms.[3]

Initial spectroscopic, structural, and reactivity studies (L = CO, 1-MeIm, CH_3CN) have suggested that these species, **1** and **2**, be regarded as copper(I) complexes but have not explained the unusual reactivity or structures.[1-3] Equilibrium binding constant studies, reported here, help to define the nature of copper binding to both axial, L, and macrocyclic ligands. This paper presents experimentally determined equilibrium constants obtained with a wide range of monodentate ligands reacting with several copper–macrocyclic ligand complexes.

Determination of Equilibrium Constants

Equilibrium constants K^I (eq 2) were measured for a variety

$$Cu^I(mac) + L \overset{K^I}{\rightleftharpoons} Cu^I(mac)(L) \qquad (2)$$

of copper(I)–macrocyclic ligand complexes, $Cu^I(mac)$, and monodentate ligands, L, in acetone or dimethylformamide (DMF). All determinations were made by using electrochemical methods. Since this technique has not been widely applied for monitoring ligand binding, a detailed description of the procedure is given here.

From the Nernst equation, eq 3, an expression can be

$$E = E^\circ + \frac{RT}{nF} \ln \frac{[Cu(II)]}{[Cu(I)]} \qquad (3)$$

derived that relates reduction potentials and copper(II) and copper(I) equilibrium binding constants. If the equilibria given in eq 4 and 6 are the only equilibria in solution, the derived

$$Cu^{II}(mac) + L \rightleftharpoons Cu^{II}(mac)(L) \qquad (4)$$

$$K^{II} = [Cu^{II}(mac)(L)]/[Cu^{II}(mac)][L] \qquad (5)$$

$$Cu^I(mac) + L \rightleftharpoons Cu^I(mac)(L) \qquad (6)$$

$$K^I = [Cu^I(mac)(L)]/[Cu^I(mac)][L] \qquad (7)$$

electrochemical relationship in eq 8 results, where $E_{1/2}(L)$ is

$$E_{1/2}(L) = E_{1/2} + \frac{RT}{nF} \ln \left[\frac{1 + K^I[L]}{1 + K^{II}[L]} \right] \qquad (8)$$

the half-wave potential measured with some monodentate ligand L present and $E_{1/2}$ is the corresponding potential in the absence of ligand. Derivation of this relationship has been described elsewhere.[4-7]

Experimentally, half-wave potentials were determined for a copper(II) solution under argon and with various concentrations of monodentate ligand L. The binding constants K^{II} and K^I were calculated by using a form of eq 8, given in eq 9

$$\frac{1}{e^{\Delta E(nF/RT)} - 1} = \frac{1}{K^I - K^{II}} \left(\frac{1}{[L]} \right) + \frac{K^{II}}{K^I - K^{II}} \qquad (9)$$

where

$$\Delta E \equiv E_{1/2}(L) - E_{1/2} \qquad (10)$$

A plot of the reciprocal of the exponential term, $e^{\Delta E(nF/RT)} - 1$, vs. the reciprocal of [L] has a slope equal to $1/(K^I - K^{II})$ and an ordinate intercept equal to $K^{II}/(K^I - K^{II})$. The binding constants K^I and K^{II} can be determined from the slope and intercept by solving simultaneous equations.

A simpler expression can be used when either $K^{II}[L]$ or $K^I[L]$ approaches zero. As $K^{II}[L]$ approaches zero, eq 8

0020-1669/79/1318-2767$01.00/0

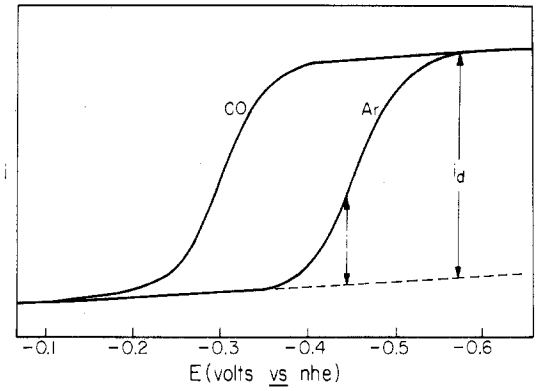

Figure 1. Sampled dc polarograms with curves smoothed of complex **4** (0.5 mM) in DMF with carbon monoxide, $E_{1/2}$ = −0.296 V, and argon, $E_{1/2}$ = −0.456 V.

Table I. Representative Sampled DC Polarographic Results for 4 and Fifth Ligands in DMF[a]

ligand, L	$10^3[L]_i$, M	I_d[b]	−slope[c]	r^2 [c]	$E_{1/2}(L)$[c]
no ligand[d]	0.0	1.70	56.8	0.9993	−0.456
p-NC(C_6H_4)NC	5.03	1.61	58.5	0.9992	−0.166
p-NO_2(C_6H_4)NC	5.08	1.69	64.5	0.9996	−0.168
$P(OC_6H_{11})_3$	1.99	1.64	81.5	0.9995	−0.251
$P(OBu)_3$	2.06	1.65	79.2	0.9995	−0.270
$P(O\text{-}p\text{-}C_6H_4Cl)_3$	2.00	1.67	59.6	0.9995	−0.304
CO	4.64	1.70	57.3	0.9997	−0.296
$P(O\text{-}p\text{-}C_6H_4CH_3)_3$	1.03	1.60	67.0	0.9999	−0.349
$P(O\text{-}o\text{-}C_6H_4CH_3)_3$	2.41	1.53	58.7	0.9998	−0.337
$P(p\text{-}C_6H_4Cl)_3$	5.00	1.56	56.9	0.9998	−0.327
	2.00	1.71	62.9	0.9998	−0.352
	0.960	1.69	67.2	0.9998	−0.375
	0.800	1.64	68.2	0.9993	−0.380
	0.640	1.70	72.1	0.9997	−0.389
$P(p\text{-}C_6H_4CH_3)_3$	2.00	1.56	64.0	0.9989	−0.360
$P(C_6H_5)_3$	2.00	1.71	62.6	0.9999	−0.363
$P(o\text{-}C_6H_4OCH_3)_3$	2.00	1.67	58.7	0.9994	−0.458
$P(o\text{-}C_6H_4CH_3)_3$	2.00	1.68	57.1	0.9995	−0.459

[a] [Cu(II)] = 5.00 × 10^{-4} M. Temperature, average value, 22 °C. Drop time, *t*, 5 s. [b] I_d, μA $s^{1/2}$ $(mM)^{-1}$ $(mg)^{-2/3}$. [c] From linear regression fit of plot of *E* vs. ln $[i/(i_d - i)]$: −slope, mV; r^2, coefficient of determination; $E_{1/2}(L)$, ordinate intercept, in volts vs. NHE, assuming $E^f_{ferrocene}$ = 0.400 V. [d] Average values.

becomes eq 11. One potential shift measurement due to a

$$e^{\Delta E(nF/RT)} - 1 = K^I[L] \qquad (11)$$

single L concentration thus allows calculation of K^I.[8]

Half-wave potentials for the reduction of copper(II) to copper(I) were evaluated from sampled dc polarograms.[8] Figure 1 shows polarograms for the copper(II) compound **4** in dimethylformamide (DMF) with argon and carbon monoxide atmospheres. The half-wave potential of a cathodic wave was evaluated by using the relationship given in eq 12, where

$$E = E_{1/2} - \frac{RT}{nF} \ln \frac{i}{i_d - i} \qquad (12)$$

i is the mean current and i_d is the mean diffusion current, measured as indicated in Figure 1. Diffusion current constants I_d, characteristic of a compound in a particular solvent, were calculated by using the measured mean diffusion current i_d and the relationship given in eq 13. In eq 13, $[Cu_B]$ is the

$$I_d = i_d/([Cu_B]m^{2/3}t^{1/6}) \qquad (13)$$

bulk concentration of electroactive species (mM), *m* is the mercury flow rate (mg/s), and *t* is the drop time (s). Half-wave potentials $E_{1/2}$ were determined as the intercepts of *E* vs. ln $[i/(i_d - i)]$ plots. Theoretically, such plots should have a slope of $-RT/nF$ for a reversible, electrochemical process. In practice the measured slopes of *E* vs. ln $[i/(i_d - i)]$ plots were used as one indication of electrochemical reversibility. Logarithmic analyses of polarograms of **4**, with added ligands at initial concentration $[L]_i$, resulted in values for I_d, slope, and $E_{1/2}(L)$, presented in Table I (DMF as solvent) and Table II (acetone as solvent). For some ligands other than $P(p\text{-}C_6H_4Cl)_3$ and pyridine a series of different ligand concentrations were examined, but the data presented are representative.

Table II. Representative Sampled DC Polarographic Results for 4 and Fifth Ligands in Acetone[a]

ligand, L	$10^3[L]_i$, M	I_d[b]	−slope[c]	r^2 [c]	$E_{1/2}(L)$[c]
no ligand[d]	0.0	2.93	59.0	0.9991	−0.400
$P(OBu)_3$	2.05	2.70	59.9	0.9987	−0.168
$P(O\text{-}p\text{-}C_6H_4Cl)_3$	2.73	2.65	60.3	0.9925	−0.205
$P(C_6H_5)_3$	3.18	2.57	57.6	0.9999	−0.270
py	100.4	2.78	57.3	0.9994	−0.462
	50.8	2.83	58.3	0.9990	−0.450
	33.5	2.81	58.0	0.9995	−0.440
	25.4	2.81	58.7	0.9995	−0.435
	20.3	2.80	58.0	0.9993	−0.431
	16.7	2.78	57.3	0.9991	−0.427
4-$(CH_3)_2$N(py)	100.0	2.62	59.9	0.9994	−0.532
$(CH_3)_2N(C_6H_5)$	50.5	2.64	54.8	0.9995	−0.401
4-CH_3O_2C(py)	116.9	2.60	56.9	0.9997	−0.434

[a] [Cu(II)] = 4.99 × 10^{-4} M. Temperature, average value, 22 °C. Drop time, *t*, 5 s. [b] I_d, μA $s^{1/2}$ $(mM)^{-1}$ $(mg)^{-2/3}$. [c] From linear regression fit of plot of *E* vs. ln $[i/(i_d - i)]$: −slope, mV; r^2, coefficient of determination; $E_{1/2}(L)$, ordinate intercept, in volts vs. NHE, assuming $E^f_{ferrocene}$ = +0.400 V. [d] Average values.

The negative slope should be 58.6 mV at 22 °C for $n = 1$. For the reduction of copper(II) to copper(I) in the presence of ligand L negative slopes varying from 54.8 to 81.5 mV were found, Table I. The majority of slopes are close to 58.6 mV consistent with electrochemically reversible reduction processes. The glaring exceptions (in DMF) are $P(OBu)_3$ (−79.2 mV), $P(OC_6H_{11})_3$ (−81.5 mV), and $P(p\text{-}C_6H_4Cl)_3$ at low $[L]_i$ (−67.2 to −72.1 mV). At low $[L]_i$ or at very high K^I a problem exists which is mirrored by the slope value. If the reduction process is reversible without L, on addition of L, a reversible process will occur only if there is a sufficient excess of L to effectively maintain the electrode surface concentration, $[L]_s$, at the initial level, $[L]_i$, throughout the polarographic run. For ligands which bind especially strongly to Cu(I) a high concentration of L was necessary to maintain $[L]_s$ effectively constant throughout the reduction. Unfortunately, measuring the current *i* from plots of *E* vs. ln $[i/(i_d - i)]$ was difficult for higher concentrations due to background current problems (discussed below) so that polarograms at higher concentrations could not be quantitatively analyzed. This may account for the large negative slopes of certain logarithmic plots, viz., those of the strongly binding phosphites $P(OBu)_3$ and $P(OC_6H_{11})_3$. The data for $P(p\text{-}C_6H_4Cl)_3$, Table I, illustrate the gradual approach of the negative slope to 58.6 mV with increasing ligand concentration.

Low concentrations of phosphine ligands were used due to background currents that increase with increasing ligand concentrations. Even with only 2 mM ligand, the polarogram of $P(p\text{-}C_6H_4CH_3)_3$ had nonparallel background and diffusion currents. The background current had a greater slope (i/E) initially due to the current from an oxidation wave of the ligand,[7,9] which did not affect the more negative diffusion current of the copper(II) reduction. With increased ligand concentration, the very rapidly growing background current began to overwhelm the slope of the copper(II) reduction, and accurate determination of the half-wave potential became difficult. Low concentrations of L were used to minimize the background current slope.

Table III. Iterative Results for 4 and $P(p\text{-}C_6H_4Cl)_3$ in DMF[a]

$10^3[L]_i$,[b] M	$e^{\Delta E(nF/RT)} - 1$[c]	$10^{-4}K^I_i$,[d] M^{-1}	$10^3[L]_f$,[b] M	$10^{-4}K^I_f$,[d] M^{-1}
5.00	158.3	3.17	4.74	3.33
2.00	58.63	2.93	1.75	3.34
0.960	23.15	2.41	0.720	3.21
0.800	18.84	2.35	0.563	3.35
0.640	12.93	2.02	0.408	3.17

[a] For the reaction

$$Cu^I(mac)\ (1) + P(p\text{-}C_6H_4Cl)_3 \overset{K^I}{\rightleftharpoons} Cu^I(mac)[P(p\text{-}C_6H_4Cl)_3]$$

[b] $[L]_i$ and $[L]_f$ are initial and final L concentrations, respectively. [c] $\Delta E \equiv E_{1/2}(L) - E_{1/2}$. [d] K^I_i and K^I_f are initial and final equilibrium constants, respectively. $K^I_{i,f} = (e^{\Delta E(nF/RT)} - 1)/[L]_{i,f}$.

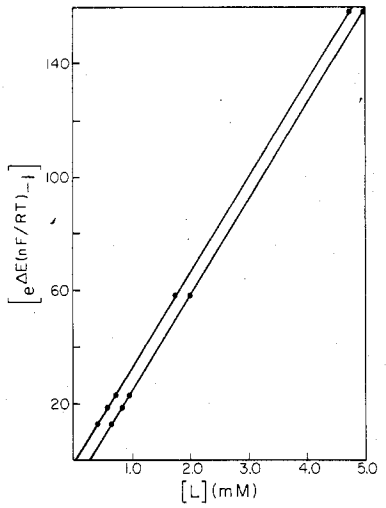

Figure 2. Graph of $e^{\Delta E(nF/RT)} - 1$ vs. [L] for five concentrations of $P(p\text{-}C_6H_4Cl)_3$ in DMF with 0.5 mM complex **4**. $\Delta E \equiv E_{1/2}[P(n\text{-}C_6H_4Cl)_3] - E_{1/2}$. The top line is the plot using $[L]_f$, the corrected ligand concentration. The slope is 3.34×10^4 M^{-1}, the ordinate intercept is −0.42, and r^2 is 0.9999. The lower line is the plot using $[L]_i$, the initial ligand concentration. The slope is 3.33×10^4 M^{-1}, the ordinate intercept is −8.29, and r^2 is 0.9999.

Problematically, however, low ligand L concentrations led to variation in the slopes of the E vs. ln $[i/(i_d - i)]$ plots from −58.6 mV and also inaccuracy in $E_{1/2}$ determinations (Table I). The value of $[L]_s$ at equilibrium is not equal to the bulk or initial concentration of L, $[L]_i$, but is lowered by χ, the concentration of Cu^IL formed (eq 6 and 14). With $[L]_i$ and

$$Cu^I(mac) + L \rightleftharpoons Cu^I(mac)(L) \qquad (6)$$

$$K^I = \chi/([Cu(I)]_i - \chi)([L]_i - \chi) \qquad (14)$$

ΔE, an initial equilibrium constant K^I_i, was calculated (eq 11). This constant, K^I_i, and $[L]_i$ were used to initiate an iterative calculation of χ. The equilibrium or final concentration of L within the diffusion layer, $[L]_f$, is equal to $[L]_i$ minus the converged value of χ. This value was used to determine K^I_f, the final equilibrium constant.

The calculated $[L]_f$ values for five concentrations of $P(p\text{-}C_6H_4Cl)_3$ are given in Table III. Figure 2 graphically illustrates the difference between $[L]_i$ and $[L]_f$ in a plot of $e^{\Delta E(nF/RT)} - 1$ vs. [L] (see eq 11). The calculated ordinate intercepts of the two plots are −8.29 ($[L]_i$) and −0.42 ($[L]_f$). For any ligand at [L] = 0, ΔE is zero and the plot should pass through the origin. The use of $[L]_f$ adjusted the ordinate intercept closer to zero, the minimal change in slope ($(3.33\text{–}3.34) \times 10^4$ M^{-1}).

The other difficulty encountered with low concentrations of ligand was ambiguity in the position of the half-wave potential. The $E_{1/2}$ values determined from E vs. ln $[i/(i_d - i)]$ plots and $[L]_f$ values calculated iteratively were used to find K^I_f (eq 11). When several initial concentrations of L were examined, a plot of $e^{\Delta E(nF/RT)} - 1$ vs. $[L]_f$ (as in Figure 2) was constructed and the slope, equal to K^I_f, was determined. The coefficient of determination, r^2, is an indication of the linearity of the data pairs. Table IV condenses the results of both simple calculations of K^I from a single ΔE,$[L]_f$ pair and the linear regression calculations of slopes, intercepts, and coefficients of determination for a series of ΔE,$[L]_f$ pairs. With the assumption that K^{II} is zero, K^I values were calculated and the r^2 values indicate a good data fit (Table IV). Because of the correlation of high and low ligand concentration data, the error in determination of $E_{1/2}$ appears to be smaller than the theoretically predicted error, $\Delta E'$ (eq 15).[7] The error, $\Delta E'$,

$$\Delta E' \approx RT[Cu(II)]/(2nF[L]) \qquad (15)$$

is ±0.0015 V with $[Cu(II)] = 5 \times 10^{-4}$ M and $[L] = 2 \times 10^{-3}$ M. An error of ±0.0025 V in $E_{1/2}(L)$ has been estimated, corresponding to $[L] = 1.25 \times 10^{-3}$ M or, as intended, large enough to include instrumental and technique errors at all L concentrations.

With an estimation of error in $E_{1/2}(L)$ the question of equilibrium binding constant values can be addressed. Equilibrium constants were evaluated by using the assumptions

Table IV. Determination of Equilibrium Binding Constants K^I with the Assumption $K^{II} = 0$[a]

ligand, L	solvent	pts[b]	r^2 [c]	b[c]	K^I,[a,c,d] M^{-1}
$p\text{-}NC(C_6H_4)NC$	DMF	3	0.9994	−2500	1.9×10^7
$p\text{-}NO_2(C_6H_4)NC$	DMF	3	0.9996	−620	1.7×10^7
$P(OC_6H_{11})_3$	DMF	2			1.8×10^6
$P(OBu)_3$	DMF	2			8.3×10^5
	acetone	2			5.1×10^6
$P(O\text{-}p\text{-}C_6H_4Cl)_3$	DMF	5	0.9997	8.6	2.2×10^5
	acetone	2			8.6×10^5
CO	DMF	2			1.2×10^5
$P(OC_6H_5)_3$	DMF	5	0.9960	−2.6	1.1×10^5
$P(O\text{-}p\text{-}C_6H_4CH_3)_3$	DMF	4	0.9946	0.74	8.7×10^4
$P(O\text{-}o\text{-}C_6H_4CH_3)_3$	DMF	2			4.9×10^4
$P(p\text{-}C_6H_4Cl)_3$	DMF	6	0.9999	−0.60	3.3×10^4
$P(p\text{-}C_6H_4CH_3)_3$	DMF	5	0.9986	−0.66	2.4×10^4
$P(C_6H_5)_3$	DMF	5	0.9984	0.59	2.1×10^4
	acetone	2			5.6×10^4
$P(o\text{-}C_6H_4OCH_3)_3$	DMF	2			0
$P(o\text{-}C_6H_4CH_3)_3$	DMF	2			0

[a] For the reactions

$$Cu^I(mac)\ (1) + L \overset{K^I}{\rightleftharpoons} Cu^I(mac)(L)$$

$$Cu^{II}(mac)^+\ (4) + L \overset{K^{II}}{\rightleftharpoons} Cu^{II}(mac)(L)^+$$

[b] Number of ΔE, [L] points used to determine K^I. This number includes (0, 0) which was used in each K^I calculation. [c] Plot of $e^{\Delta E(nF/RT)} - 1$ vs. [L]; $\Delta E = E_{1/2}(L) - E_{1/2}$. Coefficient of determination = r^2, ordinate intercept = b, slope = K^I. [d] $K^I = 0$ indicates an equilibrium constant ≤10.

Table V. Determination of Equilibrium Binding Constants K^{II} for **4** with the Assumption $K^{I} = 0$[a]

ligand, L	solvent	pts[b]	r^2 [c]	b[c]	K^{II},[c,d] M^{-1}
$P(o\text{-}C_6H_4OCH_3)_3$	DMF	2			4.1×10
$P(o\text{-}C_6H_4CH_3)_3$	DMF	2			6.4×10
py	acetone	7	0.9929	0.24	1.0×10^2
$4\text{-}(CH_3)_2N(py)$	acetone	7	0.9901	28.00	1.6×10^3
$(CH_3)_2N(C_6H_5)$	acetone	2			0
$4\text{-}CH_3O_2C(py)$	acetone	6	0.9926	−0.09	2.7×10

[a] For the reactions

$$Cu^{I}(mac)\ (1) + L \overset{K^{I}}{\rightleftharpoons} Cu^{I}(mac)(L)$$

$$Cu^{II}(mac)^{+}\ (4) + L \overset{K^{II}}{\rightleftharpoons} Cu^{II}(mac)(L)^{+}$$

[b] Number of ΔE, [L] points used to determine K^{I}. This number includes (0, 0) which was used in each K^{II} calculation. [c] Plot of $e^{\Delta E(nF/RT)} - 1$ vs. [L]; $\Delta E = E_{1/2}(L) - E_{1/2}$. Coefficient of determination = r^2, ordinate intercept = b, slope = K^{II}. [d] $K^{II} = 0$ indicates an equilibrium constant ≤ 10.

Table VI. Determination of Equilibrium Constants K^{I} and K^{II} for **4**[a]

ligand, L	solvent	pts[b]	r^2 [c]	K^{I},[c] M^{-1}	K^{II},[c] M^{-1}
$P(O\text{-}p\text{-}C_6H_4Cl)_3$	DMF	4	0.9977	2.5×10^5	2.2×10
$4\text{-}(CH_3)_2N(py)$	acetone	6	0.9815	1.5×10	4.3×10^3

[a] For the reactions

$$Cu^{I}(mac)\ (1) + L \overset{K^{I}}{\rightleftharpoons} Cu^{I}(mac)(L)$$

$$Cu^{II}(mac)^{+}\ (4) + L \overset{K^{II}}{\rightleftharpoons} Cu^{II}(mac)(L)^{+}$$

[b] Number of ΔE, [L] points used to determine K^{I} and K^{II}. The point (0, 0) was not used in these calculations. [c] Plot of $1/(e^{\Delta E(nF/RT)} - 1)$ vs. $1/[L]$; $\Delta E = E_{1/2}(L) - E_{1/2}$. For $K^{I} > K^{II}$, ordinate intercept = $K^{II}/(K^{I} - K^{II})$ and slope = $1/(K^{I} - K^{II})$. For $K^{II} > K^{I}$, ordinate intercept = $K^{I}/(K^{II} - K^{I})$ and slope = $1/(K^{II} - K^{I})$. Coefficient of determination = r^2.

$K^{II} = 0$ (Table IV) and $K^{I} = 0$ (Table V). Equation 16 was

$$e^{\Delta E(nF/RT)} - 1 = K^{I,II}{}_{f}[L]_{f} \qquad (16)$$

used, with $\Delta E = |E_{1/2}(L) - E_{1/2}|$, to calculate either K^{I} or K^{II}. Each calculation included the point (0, 0) and the linearity of all the points is indicated by the coefficient of determination, r^2, and the closeness of the ordinate intercept to zero. The fit was good in most cases. In only two cases were the data better fit by removal of the assumption that K^{I} or K^{II} is equal to zero. These cases are given in Table VI with the binding constant values, calculated by using eq 9. Finally, Table VII summarizes the best-fit K^{I} and K^{II} values with errors (error in $E_{1/2}(L) = \pm 0.0025$ V).

Four-coordinate copper(I)–macrocyclic ligand complexes other than **1** were found to also bind monodentate ligands L to form five-coordinate adducts. Electrochemical measurements were used to study the binding of carbon monoxide and of $p\text{-}NO_2(C_6H_4)NC$ with various copper complexes. Collection and analysis of electrochemical data were performed as described in detail for **4**. Table VIII presents the resulting equilibrium constants for the binding of carbon monoxide to various copper(I) complexes in DMF, along with data from other sources. Table IX presents equilibrium constants found for the reaction of $p\text{-}NO_2(C_6H_4)NC$ with five copper(I) complexes in DMF. The copper(II) complexes are depicted in Chart I.

Discussion

Methods. Previous investigations demonstrated the ability of the distorted square-planar copper(I) complex **1** to bind

Table VII. Final Equilibrium Constants of Ligands with **4**

ligand, L	solvent	K^{I},[a-c] M^{-1}	K^{II},[b-d] M^{-1}
$p\text{-}NC(C_6H_4)NC$	DMF	$1.9\ (4) \times 10^7$ [e]	0
$p\text{-}NO_2(C_6H_4)NC$	DMF	$1.7\ (2) \times 10^7$	0
$P(OC_6H_{11})_3$	DMF	$1.8\ (2) \times 10^6$	0
$P(OBu)_3$	DMF	$8.3\ (8) \times 10^5$	0
	acetone	$5.1\ (5) \times 10^6$	0
$P(O\text{-}p\text{-}C_6H_4Cl)_3$	DMF	$2.5\ (3) \times 10^5$	$2.2\ (3) \times 10$
	acetone	$8.6\ (9) \times 10^5$	0
CO	DMF	$1.2\ (2) \times 10^5$	0
$P(OC_6H_5)_3$	DMF	$1.1\ (2) \times 10^5$	0
$P(O\text{-}p\text{-}C_6H_4CH_3)_3$	DMF	$8.7\ (10) \times 10^4$	0
$P(O\text{-}o\text{-}C_6H_4CH_3)_3$	DMF	$4.9\ (5) \times 10^4$	0
$P(p\text{-}C_6H_4Cl)_3$	DMF	$3.3\ (4) \times 10^4$	0
$P(p\text{-}C_6H_4CH_3)_3$	DMF	$2.4\ (3) \times 10^4$	0
$P(C_6H_5)_3$	DMF	$2.1\ (3) \times 10^4$	0
	acetone	$5.6\ (6) \times 10^4$	0
$P(o\text{-}C_6H_4OCH_3)_3$	DMF	0	$4\ (6) \times 10$
$P(o\text{-}C_6H_4CH_3)_3$	DMF	0	$6\ (6) \times 10$
$(CH_3)_2N(C_6H_5)$	acetone	0	0
py	acetone	0	$1.0\ (3) \times 10^2$
$4\text{-}(CH_3)_2N(py)$	acetone	$1.5\ (2) \times 10$	$4.3\ (4) \times 10^3$
$4\text{-}CH_3O_2C(py)$	acetone	0	$2.7\ (8) \times 10$

[a] For the reaction

$$Cu^{I}(mac)\ (1) + L \overset{K^{I}}{\rightleftharpoons} Cu^{I}(mac)(L)$$

[b] K^{I}, $K^{II} = 0$ indicates an equilibrium constant ≤ 10. [c] Bonding is assumed to have been through carbon since $NC(C_6H_5)$ at 3×10^{-2} M did not shift the copper reduction wave in DMF. [d] For the reaction

$$Cu^{II}(mac)^{+}\ (4) + L \overset{K^{II}}{\rightleftharpoons} Cu^{II}(mac)(L)^{+}$$

[e] Values in parentheses represent estimated standard deviations.

Table VIII. Equilibrium Binding Constants of Various Copper Complexes in DMF for the Reaction

$$Cu^{I}(mac)^{n+} + CO \overset{K^{I}}{\rightleftharpoons} Cu^{I}(mac)(CO)^{n+}$$

complex	$E_{1/2}$[a]	K^{I},[b] M^{-1}	ref
5	−1.303	$2.6\ (3) \times 10^3$	10
6	−1.191	$4.7\ (30) \times 10$	10
7	−1.099	$2.1\ (3) \times 10^3$	10
8	−0.656	$4.7\ (30) \times 10$	*c*
9	−0.614	$5.8\ (30) \times 10$	*c*
10	−0.517[d]	$3.1\ (3) \times 10^4$	12, 13
4	−0.456	$1.2\ (2) \times 10^5$	*c*
11	−0.438	$8.8\ (9) \times 10^5$	*c*
12	−0.404	$4.2\ (30) \times 10$	*c*
13	−0.270	$1.2\ (2) \times 10^3$	*c*
14	−0.169	$5.3\ (5) \times 10^3$	*c*
15	−0.010	0	*c*

[a] Potentials are given in volts vs. NHE, assuming $E^{f}_{ferrocene} = +0.400$ V. [b] Errors are based on an $E_{1/2}(L)$ error of ±2.5 mV. [c] This work. [d] $E_{1/2}$ is for the process $Cu^{II}Cu^{II}(mac)^{2+} + e^{-} \rightleftharpoons Cu^{II}Cu^{I}(mac)^{+}$; K^{I} is for the process $Cu^{II}Cu^{I}(mac)^{+} + CO \rightleftharpoons Cu^{II}Cu^{I}(mac)(CO)^{+}$.

Table IX. Equilibrium Binding Constants of Five Copper Complexes in DMF for the Reaction

$$Cu^{I}(mac)^{n+} + p\text{-}NO_2(C_6H_4)NC \overset{K^{I}}{\rightleftharpoons} Cu^{I}(mac)(p\text{-}NO_2(C_6H_4)NC)^{n+}$$

complex	$E_{1/2}$[a]	K^{I},[b,c] M^{-1}
8	−0.656	$1.3\ (2) \times 10^4$
9	−0.614	$8.2\ (8) \times 10^3$
4	−0.456	$1.7\ (2) \times 10^7$
12	−0.404	$7.6\ (7) \times 10^4$
15	−0.010	0

[a] Potentials are given in volts vs. NHE, assuming $E^{f}_{ferrocene} = 0.400$ V. [b] Errors are based on an $E_{1/2}(L)$ error of ±2.5 mV. [c] $K^{I} = 0$ indicates an equilibrium constant ≤ 10.

Chart I

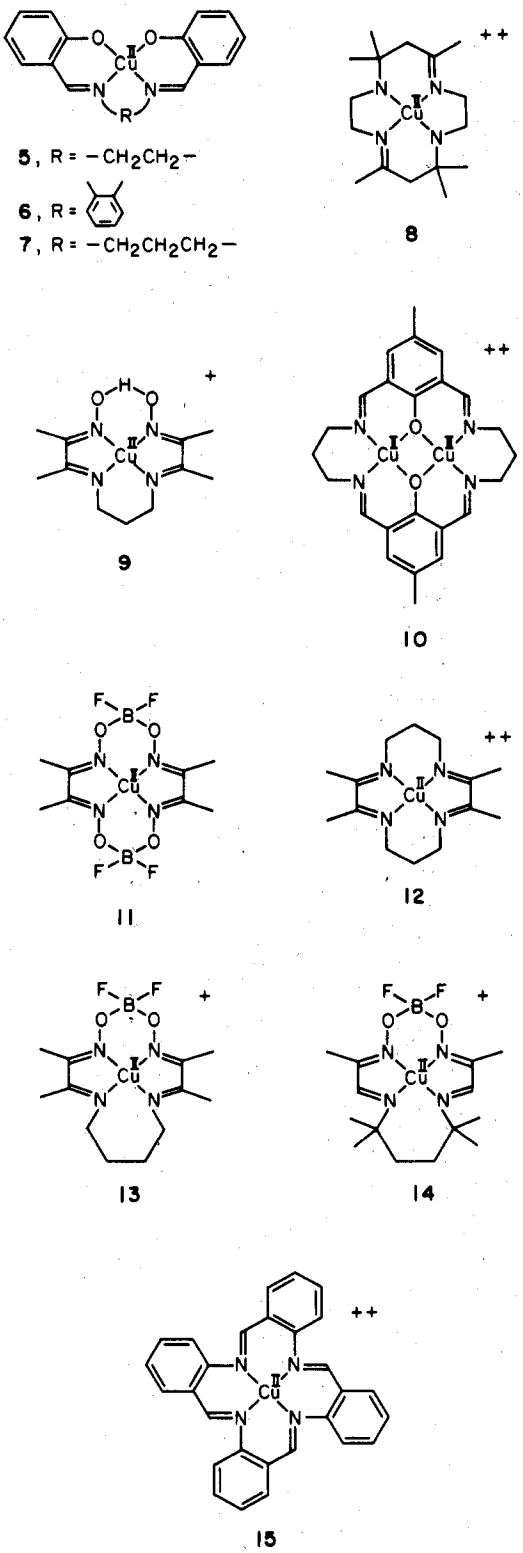

monodentate ligands (CO, 1-methylimidazole, CH_3CN, pyridine, CN^-) forming five-coordinate adducts, **2** (eq 1).[1-4] For carbon monoxide in acetone comparable equilibrium binding constants K^I, eq 2, were obtained by using both electrochemical ($K^I = 6.7 \times 10^4\ M^{-1}$) and spectral ($K^I = 4.7 \times 10^4\ M^{-1}$) techniques.[3] Spectral measurements required the isolation of pure copper(I) complex **1**, whereas the electrochemical technique utilized the copper(II) species **4**. The electrochemical method entailed, simply, measurement of the copper(II)/copper(I) reduction potential first in the absence of coordinating monodentate ligands ($E_{1/2}$) and then with varying concentrations of ligands ($E_{1/2}(L)$).

The present study has relied on electrochemical measurements to measure equilibrium binding constants (eq 2) for a variety of complexes and monodentate ligands. The binding of 18 different monodentate ligands L to the copper(II)/copper(I) redox pair **4** and **1** has been studied (Table VII). Equilibrium constants have also been determined for CO and p-$NO_2(C_6H_4)NC$ binding to several other copper(I)–macrocyclic ligand complexes (Tables VIII and IX).

These extensive studies manifest several advantages of electrochemically auditing metal–ligand interactions. Many copper(I) complexes are sensitive to dioxygen and many are not solution stable, disproportionating rapidly. The electrochemical technique permitted facile use of copper(II) complexes, requiring only that the redox processes be quasi-reversible and that copper(I) be stable as a transient species in the absence of dioxygen.[8] Indeed, we have been unable to isolate several copper(I) derivatives, including those of complexes **5–7**, due to disproportionation complications, yet electrochemical measurements have resulted in estimated copper(I) equilibrium constants. The electrochemical technique was also useful, of course, when copper(II) complexes were more readily available than the copper(I) analogues. Finally, equilibrium constants for both copper(II) and copper(I) could be extracted from a single set of measurements.

The electrochemical technique also has its shortcomings. Precision was found to be limited, as indicated in Tables VII–IX, especially with small equilibrium constants ($K < 10^2\ M^{-1}$). Large equilibrium constants ($K > 10^5\ M^{-1}$) also presented problems. The mathematical analysis utilized assumed that the concentration of ligand L did not change as copper(I) was produced and reacted with L. For large equilibrium constants a more complex, iterative computation was necessary. Presumably, larger equilibrium constants would prove even more troublesome. Finally, but perhaps most limiting, the redox species involved had to exhibit at least quasi-reversible electrochemical redox processes. The electrochemical technique has probably proved adequate for these studies since only a single bond, the copper to axial ligand bond, is involved. Moreover the rate of bond making and breaking was, apparently, sufficiently rapid that equilibrium could be approached during the course of the electrochemical measurement.[8] The entire electrochemical approach to measuring equilibrium constants, as described herein, is based on the assumption that the only two equilibria occurring in solution are represented by eq 4 and 6. This assumption would probably be invalid for substitution-labile copper(I) and copper(II) if nonpolydentate ligand complexes were involved. Conversely, monitoring reactions which achieve equilibrium only slowly would be difficult.

Equilibrium Constants. Two salient conclusions can be drawn from the equilibrium constants given in Tables VII–IX. First, the four-coordinate copper(I) complex **1** can bind various monodentate ligands other than CO, forming five-coordinate adducts. Secondly, five-coordination for copper(I) appears to be not limited to adducts of complex **1** but rather is accessible from a variety of four-coordinate copper(I) species.

A more detailed inspection of the measured equilibrium constants may afford some insight into the nature of bonding in five-coordinate copper(I). It should be noted, however, that although equilibrium constants may reflect changes in the copper–ligand (L) bond strength, they are also a function of other geometrical and solvation changes which occur on adduct formation (eq 2). Direct comparison of two equilibrium constants is not invalid but the analysis of observed trends may be more meaningful.

Reactions with Complex 1. The equilibrium constants listed in Table VII suggest that the prime requirement for strong

ligand binding by L to complex **1**, eq 1, appears to be that L be a good π acid. The strongest π acids studied, substituted phenyl isocyanides, exhibit the highest equilibrium constants, $\sim 10^7$ M^{-1}. Amines, including 1-methylimidazole (1-MeIm), are regarded as poor π acids and they have been found to bind only weakly ($K \approx 16$ M^{-1} for 1-MeIm). Pyridine and methyl isonicotinate may bind but the equilibrium constants are smaller than the experimental error of the electrochemical technique ($K < 10$ M^{-1}). Carbon monoxide and phosphites, regarded as good π acids, have been found to exhibit equilibrium constants in the medium range 10^4–10^6 M^{-1}, with phosphines binding more weakly ($\sim 10^4$ M^{-1}).

The overall order of equilibrium constants suggests that complex **1** binds better to π acceptors than to σ bases. In addition, it may be possible to discriminate between certain steric and electronic effects in binding phosphines or phosphite to the four-coordinate complex **1**.

Crystallographic analysis[3] of the carbonyl adduct of complex **1** shows the copper displaced 0.96 Å out of the mean plane of the four coordinated nitrogen atoms. The macrocyclic ligand assumes a boat conformation with the BF_2 bridge and a methylene of the propyl bridge extending upward toward copper and CO. Bulky ligands such as $P(o\text{-}C_6H_4OCH_3)_3$ and $P(o\text{-}C_6H_4CH_3)_3$ may not bind due to steric interactions with the macrocyclic ligand. By the same token, steric hindrance may account for the poorer binding of $P(O\text{-}o\text{-}C_6H_4CH_3)_3$ vs. $P(O\text{-}p\text{-}C_6H_4CH_3)_3$ and $P(o\text{-}C_6H_4CH_3)_3$ vs. $P(p\text{-}C_6H_4CH_3)_3$. In contrast, steric concerns are probably minor for para-substituted phenyl phosphite and phosphine ligands. For such ligands substituent effects may be primarily electronic in nature. Thus substituents which either increase the π acidity or decrease the σ basicity of a ligand apparently promote larger equilibrium constants K^I for binding to complex **1**.[14]

The copper(II) binding constants (Table VII) follow the expected σ-base order: $4\text{-}(CH_3)_2N(py) > py > 4\text{-}CH_3O_2C(py)$. The binding of $4\text{-}(CH_3)_2N(py)$ to copper(II) appears to be strictly through the pyridine nitrogen since the potential ligand $(CH_3)_2N(C_6H_5)$ did not shift the copper(II) reduction potential in acetone. The equilibrium constants correlate with para Hammett constants $\sigma_p^{+,-}$ for $N(CH_3)_2$, H, and CO_2CH_3.[16] The plot of log K^{II} vs. $\sigma_p^{+,-}$ has a ρ factor of -0.932 and an $r^2 = 0.9991$. The negative ρ factor indicates a reaction in which electron-donating substituents increase the equilibrium constant. Weak binding to copper(II) was found for $P(O\text{-}p\text{-}C_6H_4Cl)_3$, $K^{II} = 2.2\ (3) \times 10$ M^{-1}, which is insignificant relative to K^I [$2.5\ (3) \times 10^5$ M^{-1}].

The overall ligand binding trends indicate that copper(II) binds better to σ bases and copper(I) binds better to π acceptors. Furthermore, the copper(I) binding constants measured indicate that other ligands bind to complex **1**, as well as carbon monoxide. If the copper–carbon bond is a covalent bond with π character, as suggested earlier,[1-3] the copper–ligand bonds may have similar covalent character.

Reactions with Other Copper(I) Complexes. The most significant conclusion to be drawn from the measured equilibrium constants K^I for the copper(I) forms of complexes **5–15** (Tables VIII and IX) is that a host of copper(I)–polydentate ligand complexes apparently form five-coordinate adducts. There appears to be no basis for the notion that there is some unique feature of complex **1** which promotes five-coordination for copper(I).

The complexes examined exhibit a range of reduction potentials $E_{1/2}$ from -0.01 V to -1.3 V vs. NHE (Table VIII). For the most part the range and order of these reduction potentials can be explained. Patterson and Holm have shown that rigidly planar structures and oxygen ligands tend to favor copper(II).[17] Busch has demonstrated that increased ligand unsaturation favors lower oxidation states.[18] The salicylaldehyde derivatives **5–7** are the most difficult to reduce, presumably due to the presence of oxygen ligands and the resulting negative charge for copper(I). Complexes **8** and **10** also have relatively hard ligands but an overall positive charge, resulting in more facile reduction. Complexes **13–15** are the easiest to reduce, probably due to the flexibility of the first two, promoting tetrahedrality, and the highly delocalized nature of the TAAB ligand in **15**. The reduction potentials of complexes **4**, **11**, and **12** are curious. Despite a changing overall charge (from +1 to 0 to −1 on the copper(I) derivative) the observed values for $E_{1/2}$ are rather similar. Sterically, complexes **4**, **11**, and **12** are probably comparable, all three ligands being fairly rigid, planar moieties. The invariance in $E_{1/2}$ for **4**, **11**, and **12** may be attributable to the macrocyclic ligand charge in **4** and **11** being somewhat localized on the BF_2 bridges. Complexes **4**, as Cu(I), and **11**, as Cu(II), are neutral overall but they may be better viewed as being zwitterionic in character. The net result is that the four nitrogen ligands in **4**, **11**, and **12** probably present electronically similar coordination environments.

Comparing CO equilibrium binding constants for complexes **4**, **11**, and **12** is especially enlightening. Having sterically and electronically comparable coordination environments, as suggested above, all three complexes might be expected to exhibit similar affinities for CO. In fact, complexes **4** and **11** gave values of K^I of the same order of magnitude (1.2×10^5 M^{-1} vs. 8.8×10^5 M^{-1}, Table VIII). In contrast, complex **13** gave a much smaller value of K^I (4.2×10 M^{-1}). These differences in K^I may arise from the presence of BF_2 bridges in complexes **4** and **11**. The molecular structures of the carbonyl adducts of **4**[3] and of **11**[23] both consist of square-pyramidal coordination geometries with copper(I) displaced far out of the four-nitrogen plane (0.96 and 1.02 Å for the CO adducts of **4** and **11**, respectively). In addition, both have a fluorine of the BF_2 bridges extended toward copper, approximately 3 Å distant. That complex 12 exhibits only poor affinity for CO suggests that the BF_2 bridges in **4** and **11** may help to stabilize five-coordinate adducts by copper–fluorine interactions. Complexes **8** and **9** were examined to further test this hypothesis. As shown in Table VIII, the Cu(I) forms of complexes **8** and **9** bind CO only weakly ($K^I = 4.7 \times 10$ M^{-1} for **8**, 5.8×10 M^{-1} for **9**) despite a coordination environment and overall charge type for **9** comparable to that of complex **4**. Similar trends are seen on examining *p*-nitrophenyl isocyanide equilibrium constants (Table IX). The Cu(I) form of complex **4**, with a BF_2 bridge, binds $p\text{-}NO_2(C_6H_4)NC$ quite strongly ($K^I = 1.7 \times 10^7$ M^{-1}) but Cu(I) derivatives of **8**, **9**, and **12**, with no BF_2 bridges, exhibit significantly smaller values for K^I (8.2×10^2 to 7.6×10^4 M^{-1}). Further structural studies, presently in progress, should help to further clarify the role of the BF_2 bridge in these complexes.

It is difficult to further account for variations in the measured equilibrium constants K^I for CO or $p\text{-}NO_2(C_6H_4)NC$ binding to the copper(I) forms of **4–15**. Carbon monoxide equilibrium constants are 10^3–10^5 M^{-1} for most of the complexes studied. For these complexes variations probably reflect several factors including (a) electron density on copper(I), with high electron density promoting coordination of a π-acid ligand, (b) the geometry of the four-coordinate precursor, with square-planar structures favoring five-coordination, (c) the ability of the five-coordinate complex to assume a square-pyramidal configuration, and (d) solvation effects as they relate to the change in coordination geometry.

Summary

The four-coordinate copper(I) complex, **1**, reacts with a variety of monodentate ligands to form five-coordinate adducts. Equilibrium constants for the reaction suggest that the copper(I)–fifth ligand bond strength correlates with ligand π

acidity in the order isocyanides > phosphites ~ CO > phosphines > amines. It thus appears that metal-to-ligand π back-bonding may be a significant component of the copper(I)–fifth ligand bond.

In fact, a variety of four-coordinate copper(I) complexes apparently react with CO or p-$NO_2(C_6H_4)NC$ to form five-coordinate adducts. Five-coordination for copper(I) appears to be promoted by near square planarity for the four-coordinate precursor with yet sufficient ligand flexibility to permit distortion to a square-pyramidal coordination geometry. The presence of difluoroboron bridges on the periphery of certain macrocyclic ligands may further promote five-coordination via copper–fluorine interactions.

Experimental Section

Materials. Tetrabutylammonium perchlorate, TBAP (Southwestern Analytical Chemicals), was dried exhaustively in vacuo before use. Ferrocene was recrystallized from benzene. For electrochemical measurements DMF was dried first over $MgSO_4/CaSO_4$ and then over 4A molecular sieves and vacuum distilled. Spectroquality acetone was used for electrochemical measurements without further purification. Argon was purified by passing it first over hot copper turnings and then over 4A molecular sieves. Carbon monoxide was passed over activated Ridox and molecular sieves. Complexes **4**,[3] **5**,[18] **6**,[20] **7**,[21] **8**,[22] **10**,[12,13] **11**,[23] and **15**[24] were prepared by the methods given in the references listed. Compounds **4**, **8**, and **9** were used as the perchlorate salts. *Caution: Perchlorate salts may be explosive.* Complex **15** was used as the nitrate salt. All complexes gave satisfactory elemental analyses.

Synthesis of (2,3,9,10-Tetramethyl-1,4,8,11-tetraazacyclotetradeca-1,3,8,10-tetraene)copper(II) Diperchlorate (12). To a solution of 1,3-propanediamine (9.0 g) in methanol (300 mL) was added perchloric acid (16.7 g, 60%), followed by 2,3-butanedione (8.6 g). After 30 min of stirring at ambient temperature, $Cu^{II}(CH_3CO_2)_2 \cdot H_2O$ (10.0 g) was added. The reaction was stirred for 6 h. Perchloric acid (21.5 mL, 60%) was added. The red-brown reaction mixture was then concentrated on a rotary evaporator to a red oil containing a light precipitate. The mixture was filtered. The filtrate was diluted with H_2O (50 mL). A saturated aqueous sodium perchlorate solution (25 mL) was added. When the mixture was cooled to 2 °C, a red microcrystalline solid was obtained. Recrystallization from acetone–ethanol gave wine red needles, which were dried in vacuo. Anal. Calcd for $C_{14}H_{24}Cl_2CuN_4O_8$: C, 32.92; H, 4.74; N, 10.97; Cu, 12.44. Found: C, 33.0; H, 5.0; N, 11.0; Cu, 12.5.

4,9-Diaza-3,10-dimethyldodeca-3,9-diene-2,11-dione Dioxime (16), the Free Ligand of Complex 13. 1,4-Diaminobutane (8.82 g, 0.10 mol) was added to a refluxing solution of 2,3-butanedione oxime (20.2 g, 0.20 mol) in ethanol (75 mL). After 2 h of boiling, the solution was reduced in volume to about 50 mL. When the solution was allowed to cool to ambient temperature, a solid precipitated. The product was isolated by vacuum filtration, washed with ethanol and diethyl ether, and air-dried: yield of white product 6.7 g, 26%; ^2H NMR (Me_2SO-d_6) δ 1.67 (m, 2), 1.98 (s, 3), 2.08 (s, 3), 3.35 (m, 2), 11.28 (s, 1).

Complex 13. A hot solution of $Cu(ClO_4)_2 \cdot 6H_2O$ (3.7 g, 0.01 mol) in ethanol (20 mL) was slowly added to a hot solution of the free ligand, **16** (5.1 g, 0.02 mol), in ethanol (50 mL). The resulting red-brown solution was heated at reflux for 5 min and then cooled to ambient temperature. The resulting dark solid was isolated by vacuum filtration, washed with ethanol and diethyl ether, and recrystallized from a minimum volume of acetone. A boiling dioxane solution (50 mL) of the product (1.5 g, 3.6 mmol) was then treated with boron trifluoride etherate (5 mL, 0.04 mol) and kept at reflux for 1 h. After the solution was cooled, a light purple solid was isolated by vacuum filtration and washed with dioxane and diethyl ether. The complex was recrystallized by slowly adding dioxane to a saturated acetone solution. Anal. Calcd for $C_{14}H_{24}BClCuF_2N_4O_5$: C, 33.09; H, 4.76; N, 11.03. Found: C, 33.2; H, 4.9; N, 11.0.

Synthesis of 4,9-Diaza-5,5,8,8-tetramethyldodeca-3,9-diene-2,11-dione Dioxime (17), the Free Ligand of Complex 14. 2-Oximinopropanal (0.65 g), made from 2-oximinopropanal dimethyl acetal, was dissolved in ethanol (4 mL). To this was added 2,5-dimethyl-2,5-hexanediamine (0.50 g). The mixture was heated to reflux for 15 min. When the mixture was cooled to 2 °C, white crystals were formed. The product was isolated by filtration and washed with ether (3 mL): NMR (Me_2SO-d_6) δ 1.10 (s, 6), 1.38 (s, 2), 1.89 (s, 3), 7.76 (s, 1), 11.50 (br, 1).

Synthesis of 14. To a warm solution of **17** (0.47 g) in ethanol (4 mL) was added a warm solution of $Cu^{II}(ClO_4)_2 \cdot 6H_2O$ (0.41 g) in ethanol (4 mL). The reaction was heated gently for 15 min. When the reaction mixture was cooled to ambient temperature, a green solid was obtained. The product was recrystallized from acetone. Anal. Calcd for $C_{14}H_{25}ClCuN_4O_6$: C, 37.84; H, 5.67; N, 12.61; Cu, 14.30. Found: C, 38.1; H, 5.6; N, 12.5; Cu, 14.4.

In dioxane (10 mL), the complex above (0.31 g) was stirred with $BF_3 \cdot Et_2O$ (1.5 mL). The mixture was then heated to reflux for 30 min. The reaction was cooled to ambient temperature. The product was isolated by filtration and washed with dioxane and ether. Recrystallization was performed in acetone–ethanol to give a blue microcrystalline solid, which was dried in vacuo. Anal. Calcd for $C_{14}H_{24}BClCuF_2N_4O_6$: C, 34.16; H, 4.91; N, 11.38; Cu, 12.91. Found: C, 34.4; H, 4.9; N, 11.4; Cu, 13.4.

Electrochemistry. A Princeton Applied Research Model 174 polarographic analyzer was used for sampled dc polarography and for cyclic voltammetry. Data were recorded on a Hewlett-Packard Model 7004B X-Y recorder. A simple H-type electrochemical cell was used. The two compartments of the cell were separated by a medium-porosity sintered glass frit. The main working compartment had a three-way stopcock arrangement on a gas-inlet tube, permitting gas to be bubbled up through the solution or to simply flow above the working solution. A second stopcock at the base of the working compartment allowed the working solution to be easily changed. A dropping mercury electrode (PAR Model 9346) served as the working electrode and a platinum wire coiled around the mercury capillary served as the counterelectrode. A Ag/Ag^+ reference electrode was placed in the second compartment of the cell. The reference electrode consisted of a silver wire immersed in an acetonitrile solution of $AgNO_3$ (0.01 M) and TBAP (0.1 M), all contained in an 8-mm glass tube fitted on the bottom with a fine-porosity sintered glass frit. The silver wire was threaded through a serum cap fitted snugly over the top of the 8-mm tube.

Polarographic analyses were performed with acetone or DMF solutions containing TBAP (0.1 M) as supporting electrolyte. The working compartment also contained a copper(II) sample (0.5 mM), ferrocene (1.0 mM), and some monodentate ligand, L (zero to several millimolar). In practice, working solutions were prepared in an inert-atmosphere chamber (Vacuum Atmospheres, Inc.; filled with helium) from stock solutions of copper(II) and ferrocene. Volumetric additions of ligand were then made.

The procedure for obtaining sampled dc polarograms began and ended with a mercury flow rate measurement. Mercury flowing from the capillary into a solvent was collected with the drop knocker set at a drop time of 5 s. (All polarograms were run with $t = 5$ s.) The time over which mercury was collected was recorded. The flow rate, m, was calculated in milligrams per second. The copper(II) sample was then purged with argon for 20 min. The cyclic voltammogram of ferrocene was measured with a platinum-disk electrode with the platinum counterelectrode coiled around it. The sampled dc polarogram was run at 0.5 mV s^{-1} and the ambient temperature recorded (22 ± 1 °C).

The half-wave potential of the sample, $E_{1/2}$, was determined from an E vs. $\ln [i/(i_d - i)]$ plot. The linear regression of the plot was calculated by use of a program written for a Hewlett-Packard Model 25 programmable calculator. The intercept of the plots gave $E_{1/2}$ vs. Ag/Ag^+, with the slope being theoretically equal to $-RT/nF$.

No attempt to correct potentials measured against the Ag/Ag^+ reference electrode was made; instead ferrocene served as an internal reference redox couple. It has been proposed that the oxidation of ferrocene to ferrocenium ion occurs near the same potential in most solvents.[25] In water the process occurs at +0.400 V vs. NHE.[26] Measuring both $E^f_{ferrocene}$ and $E_{1/2}$[Cu(II/I)] under the same conditions permitted a better estimate of potentials vs. NHE because unknown junction potentials associated with the Ag/Ag^+ could be ignored. Half-wave potentials for samples, $E_{1/2}$, were determined vs. Ag/Ag^+ as described above and then corrected by using the measured $E^f_{ferrocene}$ and a value of 0.400 V vs. NHE for ferrocene; i.e., $E_{1/2}(NHE) = E_{1/2}(Ag/Ag^+) - [E^f_{ferrocene} + 0.400\ V]$. All potentials are reported vs. the NHE by using this correction.

Measurements of carbon monoxide binding were performed with DMF solutions saturated with CO at 1 atm of pressure. At this

pressure the concentration of CO in solution was taken to be 4.64 mM.[27]

Acknowledgment. We appreciate the assistance of and helpful discussions with Carl A. Koval. Financial support for this research was provided by NATO and the National Institutes of Health (Grant No. PHS 4 AM18319B-04).

Registry No. **1**, 61114-07-6; **1**·*p*-NC(C_6H_4)NC, 71171-29-4; **1**·*p*-NO_2(C_6H_4)NC, 71171-30-7; **1**·P(OC_6H_{11})$_3$, 71171-31-8; **1**·P(OBu)$_3$, 71171-32-9; **1**·P(O-*p*-C_6H_4Cl)$_3$, 71171-33-0; **1**·CO, 61128-83-4; **1**·P(OC_6H_5)$_3$, 71194-22-4; **1**·P(O-*p*-$C_6H_4CH_3$)$_3$, 71171-22-7; **1**·P(O-*o*-$C_6H_4CH_3$)$_3$, 71194-23-5; **1**·P(*p*-C_6H_4Cl)$_3$, 71194-24-6; **1**·P(*p*-$C_6H_4CH_3$)$_3$, 71171-23-8; **1**·P(C_6H_5)$_3$, 71171-24-9; **1**·P(*o*-$C_6H_4OCH_3$)$_3$, 71171-25-0; **1**·P(*o*-$C_6H_4CH_3$)$_3$, 71171-26-1; **1**·$(CH_3)_2N(C_6H_5)$, 71171-27-2; **1**·py, 66069-81-6; **1**·4-$(CH_3)_2$N(py), 71171-12-5; **1**·4-CH_3O_2C(py), 71171-13-6; **4**, 64783-09-1; **4**·*p*-NC(C_6H_4)NC, 71171-14-7; **4**·*p*-NO_2(C_6H_4)NC, 71171-15-8; **4**·P(OC_6H_{11})$_3$, 71171-16-9; **4**·P(OBu)$_3$, 71171-17-0; **4**·P(O-*p*-C_6H_4Cl)$_3$, 71171-18-1; **4**·CO, 71171-19-2; **4**·P(OC_6H_5)$_3$, 71171-20-5; **4**·P(O-*p*-$C_6H_4CH_3$)$_3$, 71171-21-6; **4**·P(O-*o*-$C_6H_4CH_3$)$_3$, 71171-03-4; **4**·P(*p*-C_6H_4Cl)$_3$, 71171-04-5; **4**·P(*p*-$C_6H_4CH_3$)$_3$, 71171-05-6; **4**·P(C_6H_5)$_3$, 71171-06-7; **4**·P(*o*-$C_6H_4OCH_3$)$_3$, 71171-07-8; **4**·P(*o*-$C_6H_4CH_3$)$_3$, 71171-08-9; **4**·$(CH_3)_2N(C_6H_5)$, 71171-09-0; **4**·py, 66070-14-2; **4**·4-$(CH_3)_2$N(py), 71171-10-3; **4**·4-CH_3O_2C(py), 71171-11-4; **8**·CO, 71170-93-9; **8**·*p*-NO_2(C_6H_4)NC, 71170-94-0; **9**·CO, 71194-20-2; **9**·*p*-NO_2(C_6H_4)NC, 71170-95-1; **11**·CO, 71170-96-2; **12**·$(ClO_4)_2$, 71170-98-4; **12**·CO, 71170-99-5; **12**·*p*-NO_2(C_6H_4)NC, 71171-00-1; **13**·ClO_4, 71171-01-2; **13**·CO, 71171-02-3; **14**·ClO_4, 71171-35-2; **14**·CO, 71171-36-3; **15**·CO, 71171-37-4; **15**·*p*-NO_2(C_6H_4)NC, 71171-38-5; **16**, 71170-91-7; **17**, 71170-92-8.

References and Notes

(1) R. R. Gagné, J. L. Allison, and G. C. Lisensky, *Inorg. Chem.*, **17**, 3563 (1978).
(2) R. R. Gagné, *J. Am. Chem. Soc.*, **98**, 6709 (1976).
(3) R. R. Gagné, J. L. Allison, R. S. Gall, and C. A. Koval, *J. Am. Chem. Soc.*, **99**, 7170 (1977).
(4) A. W. Addison, M. Carpenter, L. K.-M. Lau, and M. Wicholas, *Inorg. Chem.*, **17**, 1545 (1978).
(5) J. L. Allison, Ph.D. Thesis, California Institute of Technology, 1979.
(6) H. A. Laitinen, "Chemical Analysis", McGraw-Hill, New York, N.Y., 1960, p 286.
(7) J. Heyrovsky and J. Kuta, "Principles of Polarography", Academic Press, New York, N.Y. 1966.
(8) The use of shifts in $E_{1/2}$ to calculate equilibrium constants relies on the assumption of chemical and electrochemical reversibility. Since all of the copper complex data in this paper were obtained by using dc polarography, the only criterion for reversibility was that plots of E vs. ln $[i/(i_d - i)]$ have slopes of $-RT/nF$, i.e., 58.6 mV at 22 °C for Cu(II/I). It should be noted that previous cyclic voltammetric studies also indicated chemical reversibility for the reaction of **1** and **4** with CO and with 1-methylimidazole.[3] Complex **4** shows both reduction and oxidation cyclic voltammetric waves whether measured under argon or under CO. Under CO the oxidation peak is distorted, however, which has been interpreted as possibly indicating a slow rate of CO dissociation.[3] The slower technique of sampled dc polarography was utilized to overcome the limitation of cyclic voltammetry.
(9) G. Schiavon, S. Zecchin, G. Cogoni, and G. Bontempelli, *J. Electroanal. Chem. Interfacial Electrochem.*, **48**, 425 (1973).
(10) R. R. Gagné, C. A. Koval, and E. Kober, unpublished results. See also ref 11.
(11) C. A. Koval, Ph.D. Thesis, California Institute of Technology, 1979.
(12) R. R. Gagné, C. A. Koval, and T. J. Smith, *J. Am. Chem. Soc.*, **99**, 8367 (1977).
(13) R. R. Gagné, C. A. Koval, T. J. Smith, and M. Cimolino, *J. Am. Chem. Soc.*, **101**, 4571 (1979).
(14) Tolman has defined both a steric factor, the "ligand cone angle", and an electronic factor, the "donor–acceptor parameter", for many of these phosphines and phosphites.[15] Ligands with large (≥165°) cone angles, i.e., bulky ligands, exhibit a marked suppression of their binding constants. Ligands with small cone angles, where steric forces are small, show a direct correlation, within experimental error, between donor–acceptor parameters and the equilibrium constants K^1 for binding these ligands to complex **1**.
(15) (a) C. A. Tolman, *J. Am. Chem. Soc.*, **92**, 2953 (1970); (b) *ibid.*, **92**, 2956 (1970).
(16) A. J. Gordon and R. A. Ford, "The Chemist's Companion", Wiley, New York, N.Y., pp 144–155.
(17) G. S. Patterson and R. H. Holm, *Bioinorg. Chem.*, **4**, 257 (1975).
(18) D. H. Busch, D. G. Pillsbury, F. V. Lovecchio, A. M. Tait, Y. Hung, S. Jackels, M. C. Rakowski, W. P. Schammel, and L. Y. Martin, *ACS Symp. Ser.*, **No. 38**, 32 (1976).
(19) P. Pfeiffer, E. Breith, E. Lübble, and T. Tsumaki, *Ann. Chim. (Paris)*, **503**, 84 (1933).
(20) M. J. O'Connor, R. E. Ernst, and R. H. Holm, *J. Am. Chem. Soc.*, **90**, 4561 (1968).
(21) F. Lions and K. V. Martin, *J. Am. Chem. Soc.*, **79**, 1273 (1957).
(22) D. C. Olson and J. Vasilevskis, *Inorg. Chem.*, **10**, 463 (1971).
(23) Prepared as for **4**: R. R. Gagné, D. M. Ingle, R. P. Kreh, M. McCool, and R. E. Marsh, submitted for publication.
(24) G. A. Melson and D. H. Busch, *J. Am. Chem. Soc.*, **86**, 4834 (1964).
(25) D. Bauer and M. Breant, *Electroanal. Chem.*, **8**, 282–344 (1975).
(26) H. M. Koepp, H. Wendt, and H. Strehlow, *Z. Elektrochem.*, **64**, 483 (1960).
(27) "Properties and Uses of Dimethylformamide", Du Pont, Industrial Chemicals Dept., Wilmington, Del., 1976.

Contribution from Department of Chemistry, University of Rochester, Rochester, New York 14627, and The Institute for Molecular Science, Myodaiji, Okazaki 444, Japan

Relative Stability of Bent and Linear Coordination of the Nitrosyl Ligand in Nitrosylpentaamminecobalt(III), $Co(NH_3)_5NO^{2+}$. An ab Initio Investigation

J. OAKEY NOELL[1a] and KEIJI MOROKUMA*[1a-c]

Received October 20, 1978

The stability of the complex $Co(NH_3)_5NO^{2+}$ is investigated within the ab initio SCF framework, as a function of the angle at which the nitrosyl is coordinated. We find, in agreement with experiment, that the most stable conformer is one in which the nitrosyl bends in such a manner as to eclipse an equatorial ammonia ligand. In the implementation of an energy decomposition scheme, this is interpreted as the result of enhanced electrostatic and charge-transfer interactions attendant upon bending of the nitrosyl. The preference of an eclipsed conformer to its staggered counterpart is found to be principally due to its more favored electrostatic interaction. Other topics discussed include the length of the M–N bond in relation to other nitrosyl complexes, the origin of the large trans effect, and orbital correlations as one forms the total complex as a composite of the monomers $Co(NH_3)^{3+}$ and NO^-.

Introduction

The coordination of the nitrosyl ligand to metals of the first and second transition series is currently the subject of intense research interest in both structural and interpretive inorganic chemistry. Much of this interest spawns from the first confirmation by Ibers et al.[2a,b] of a bent coordination mode for the binding of the nitrosyl ligand to a transition metal. Since this original finding a large host of nitrosyl complexes, both bent and linear in their coordination, have been prepared and structurally characterized. Frenz and Ibers[2c] have collated these data, segregating the complexes into three classes. There is the class, denoted as linear nitrosyls, in which the M–N–O bond angle is very nearly equal to 180°. By contrast, there is a second, structurally distinct group of nitrosyls whose M–N–O angle is in the vicinity of 120°. Intermediate between these extremes, there is a third class of complexes with an angle

0020-1669/79/1318-2774$01.00/0